Helmholtz-Zentrum Dresden-Rossendorf (HZDR)

HELMHOLTZ ZENTRUM
DRESDEN ROSSENDORF

Observation of charge density waves in free-standing 1T-TaSe2 monolayers by transmission electron microscopy

Börner, P. C.; Kinyanjui, M. K.; Björkman, T.; Lehnert, T.; Krasheninnikov, A. V.; Kaiser, U.;

Originally published:

October 2018

Applied Physics Letters 113(2018), 173103

DOI: https://doi.org/10.1063/1.5052722

Perma-Link to Publication Repository of HZDR:

https://www.hzdr.de/publications/Publ-28260

Release of the secondary publication
on the basis of the German Copyright Law § 38 Section 4.

Observation of charge density waves in free-standing 1T-$TaSe_2$ monolayers by transmission electron microscopy.

P. C. Börner,[1] M. K. Kinyanjui,[1] T. Björkman,[2] T. Lehnert,[1] A. V. Krasheninnikov,[3,4] and U. Kaiser[1, a)]
[1)] *Central facility of electron microscopy, Ulm University, Albert Einstein Allee 11, 89069 Ulm, Germany*
[2)] *Physics/Department of Natural Sciences, Åbo Akademi, FI-20500 Turku, Finland*
[3)] *Institute of Ion Beam Physics and Materials Research, Helmholtz-Zentrum Dresden-Rossendorf, 01328 Dresden, Germany*
[4)] *Department of Applied Physics, Aalto University, PO Box 14100, 00076 Aalto, Finland*

(Dated: 9 October 2018)

While bulk 1T-$TaSe_2$ is characterized by a commensurate charge density wave (CCDW) state below 473 K, the stability of the CCDW state in a 1T-$TaSe_2$ monolayer, although theoretically predicted, has not been experimentally confirmed so far. As CDWs and periodic lattice distortions (PLDs) always come together, we evaluate the PLD in a 1T-$TaSe_2$ monolayer from low-voltage aberration-corrected high-resolution transmission electron microscopy (AC-HRTEM) experiments. To prevent fast degradation of 1T-$TaSe_2$ during exposure to the electron-beam, a 1T-$TaSe_2$ / graphene heterostucture was prepared. We also perform the image simulations based on atom coordinates obtained using density functional theory (DFT) calculations. From the agreement between the experimental and simulated images we confirm the stability of the CCDW/PLD in a monolayer 1T-$TaSe_2$/ graphene heterostructure at room temperature in the form of a $\sqrt{13} \times \sqrt{13}$ superstructure. At the same time, we find that in comparison to multi-layer structures the superstructure is less pronounced.

PACS numbers: 61, 64, 65, 68, 81
Keywords: CDW, PLD, 1T-$TaSe_2$, 2D materials, HRTEM

Materials with reduced dimensionality are nowadays an enormously increasing field of research, involving fundamental physics, materials science, and quantum technology. It has been predicted for instance that in graphene the quantum Hall effect can be reliably measured even at room temperature.[1] Likewise, high temperature superconductivity at interfaces and in single-layers were reported.[2,3] Moreover, some of the bulk layered materials exhibit many-body quantum state features, associated with charge density wave (CDW) ordering and gap in the electronic spectrum.[4–6]

CDWs are periodic modulations of the electron charge density observed preferably in low-dimensional metals, which depend on temperature, dimensionality, doping and pressure. They often arise due to instabilities at the Fermi surface and give rise to metal-to-insulator transitions due to the opening of a band gap.[7,8] Due to electron-phonon coupling, the CDW state is always accompanied by a periodic lattice distortion (PLD) which is characterized by a periodic modulation of the atomic positions.[9] Thus, CDW and PLD always come together, and we will call them CDW/PLD throughout the paper. The CDW/PLD structure can be either commensurate or incommensurate with respect to the undistorted lattice, depending on the transition temperature and the dimensionality of the system.[4]

[a)] Electronic mail: ute.kaiser@uni-ulm.de.

Bulk transition metal dichalcogenides (TMDs) are layered materials (either semiconductors or metals) with MX_2 as the common structural formula, where M stands for transition metals, X for chalcogens S, Se, Te. The layers are coupled by van der Waals forces.[10] Thus, bulk TMDs are mechanically and electrically extremely anisotropic.[11] The possibility of obtaining single-layers from layered bulk structures[12,13] has raised great attention as many possibilities are envisaged for potential technological applications[14–16] as well as for understanding solid state quantum phenomena[4–6,10].

Bulk TMDs like $TaSe_2$, TaS_2, and $NbSe_2$ are metals that exhibit a strong CDW/PLD.[4,5] Obtaining defect-free single-layers from bulk CDW/PLD TMD materials and understanding their characteristics is an active field of research. Due to confinement effects, interesting properties are already predicted for the CDW/PLD state e.g. for single-layer 1T-TaS_2 which obtains a triclinic stripe order or for single-layer 2H-$NbSe_2$ which shows an enhanced transition temperature.[17,18] So far there are different qualitative models for the CDW phase transition e.g. the Fermi surface nesting[5,19,20], Peierls distortion[7], giant Kohn anomaly[4] but a "coherent and realistic microscopy theory has not yet emerged"[5].

For 1T-$TaSe_2$ thickness- and temperature-dependent properties have already been reported in the CCDW/PLD state: It is metallic in the bulk structure, but insulating in a single-layer,[21,22] and the transition temperature to the commensurate (C)CDW/PLD phase in the bulk structure is 437 K, which is reduced with

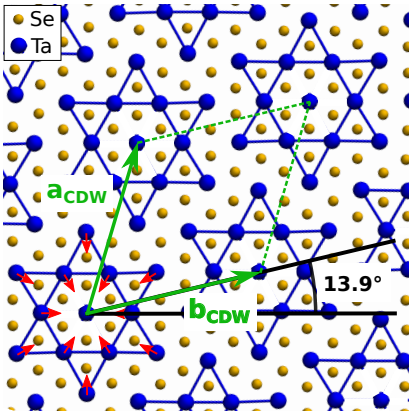

FIG. 1. Atomic structure of the CCDW/PLD in single-layer 1T-$TaSe_2$ with Ta atoms colored blue and Se atoms colored orange. The Ta atoms show a star-of-David-like superstructure consisting of 13 Ta atoms. The outer 12 Ta atoms are displaced towards the center atom, indicated by red arrows. The unit cell of the commensurate superstructure is marked with the lattice vectors $\mathbf{a_{CDW}}$ and $\mathbf{b_{CDW}}$ to show the $\sqrt{13}\,a_0 \times \sqrt{13}\,a_0$ superstructure. The superstructure is rotated about 13.9° against the undistorted 1T structure.

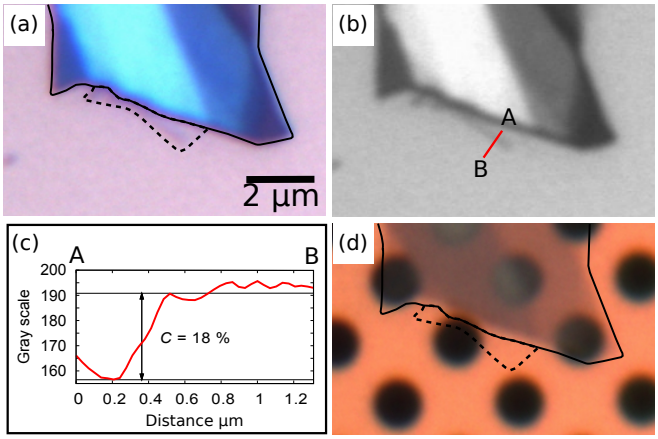

FIG. 2. Optical microscope image of a 1T-$TaSe_2$ flake on a Si/SiO_2 wafer (a). The monolayer is marked with a dashed line. The thickness of this monolayer is determined using a line scan (red) from the green-channel image (b). The profile of the line scan reveals a Weber contrast C of 18 % which identifies the layer as a monolayer. For HRTEM investigations the flake is transferred on a gold sputtered Quantifoil TEM grid with a graphene monolayer on it (d).

decreasing thickness.[23,24] However, no experimental evidence has been given for the formation of the CCDW/PLD state in freestanding monolayer 1T-$TaSe_2$ at room temperature.

In this paper we investigate the CCDW/PLD structure of free-standing single-layer 1T-$TaSe_2$ using 80 kV aberration-corrected high-resolution transmission electron microscopy (AC-HRTEM) at room temperature. The knock-on damage threshold for $TaSe_2$ is considerably higher, about (190 – 200) kV, calculated using the displacement threshold energy for Se atoms obtained within the framework of DFT-based molecular dynamics for $TaSe_2$.[25] However, previous AC-HRTEM investigations of single-layer TMDs have shown that electron beam-induced damage can lead to rapid generation of structural defects through other mechanisms, which include electronic excitations, especially for insulating materials, and beam-induced chemical etching.[26,27] The effects of electron beam-induced damage can be reduced by protecting the single-layer TMD with one graphene layer or sandwiching it between two graphene layers.[27–29] Here, we investigate the single-layer 1T-$TaSe_2$/graphene heterostructure. Furthermore, we assume that heating of a few-layer thick sample by the electron beam at 80 kV can be neglected, as experiments and theory indicate.[26,30,31]

The atomic structure of the CCDW/PLD in single-layer 1T-$TaSe_2$ is shown in Figure 1 with Ta atoms colored blue and Se atoms orange. The Ta atoms show a 13 atoms star-of-David-like pattern with a $\sqrt{13}\,a_0 \times \sqrt{13}\,a_0$ unit cell (marked in green), rotated by about 13.9° to the undistorted lattice. The superstructure lattice vectors are $\mathbf{a_{CDW}}$ and $\mathbf{b_{CDW}}$ with a length of $|\mathbf{a_{CDW}}| = |\mathbf{b_{CDW}}| = \sqrt{13}\,a_0$. The main distortion of the atoms is governed by the Ta atoms with the largest displacement of Ta being about 0.33 Å (in-plane).[5] The red arrows indicate the direction of the in-plane atom displacements. Se atoms are displaced mainly out of plane.[5] In the incommensurate (I)CDW/PLD case the rotation angle is between 0° and 13.9°, depending on the incommensurability, and a domain-like structure is formed.[5]

Single-layers of 1T-$TaSe_2$ were mechanically exfoliated from bulk material using the Scotch tape method (for more details, see supplementary).[32,33] The exact thicknesses of the 1T-$TaSe_2$ flakes were determined by contrast measurement with an optical microscope.[32,33] In Figure 2 (a), an optical microscope image of a 1T-$TaSe_2$ flake on a SiO_2 substrate is shown. The flake is marked with a black solid line and the monolayer area is marked with a dashed black line. A green channel image of the same flake is shown in Figure 2 (b) as green light is used for the contrast calculation of a 1T-$TaSe_2$ monolayer.

A line scan from A to B for the thickness determination is also indicated with a red line. The profile of the line scan is depicted in Figure 2 (c). The average values for the minimum and maximum are drawn as horizontal lines in the graph. The measured contrast is $C = 18\,\%$. This experimental value was compared to the calculated contrast for a 1T-$TaSe_2$ monolayer on SiO_2, which was conducted analogously to contrast calculations for monolayers of graphene or TMDs.[32,33] The calculated contrast C for a single 1T-$TaSe_2$ layer on this Si/SiO_2 wafer was $C = 0.19(5)$ (values for calculation, see supplementary). The confidence interval (brackets) was calculated from the propagation of the uncertainties of the physical quantities. Thus, we conclude that the layer marked with a dashed line in Figure 2 (a) is a monolayer. For HRTEM investigations, this 1T-$TaSe_2$ flake was transferred to a gold sputtered Quantifoil grid on which a graphene flake

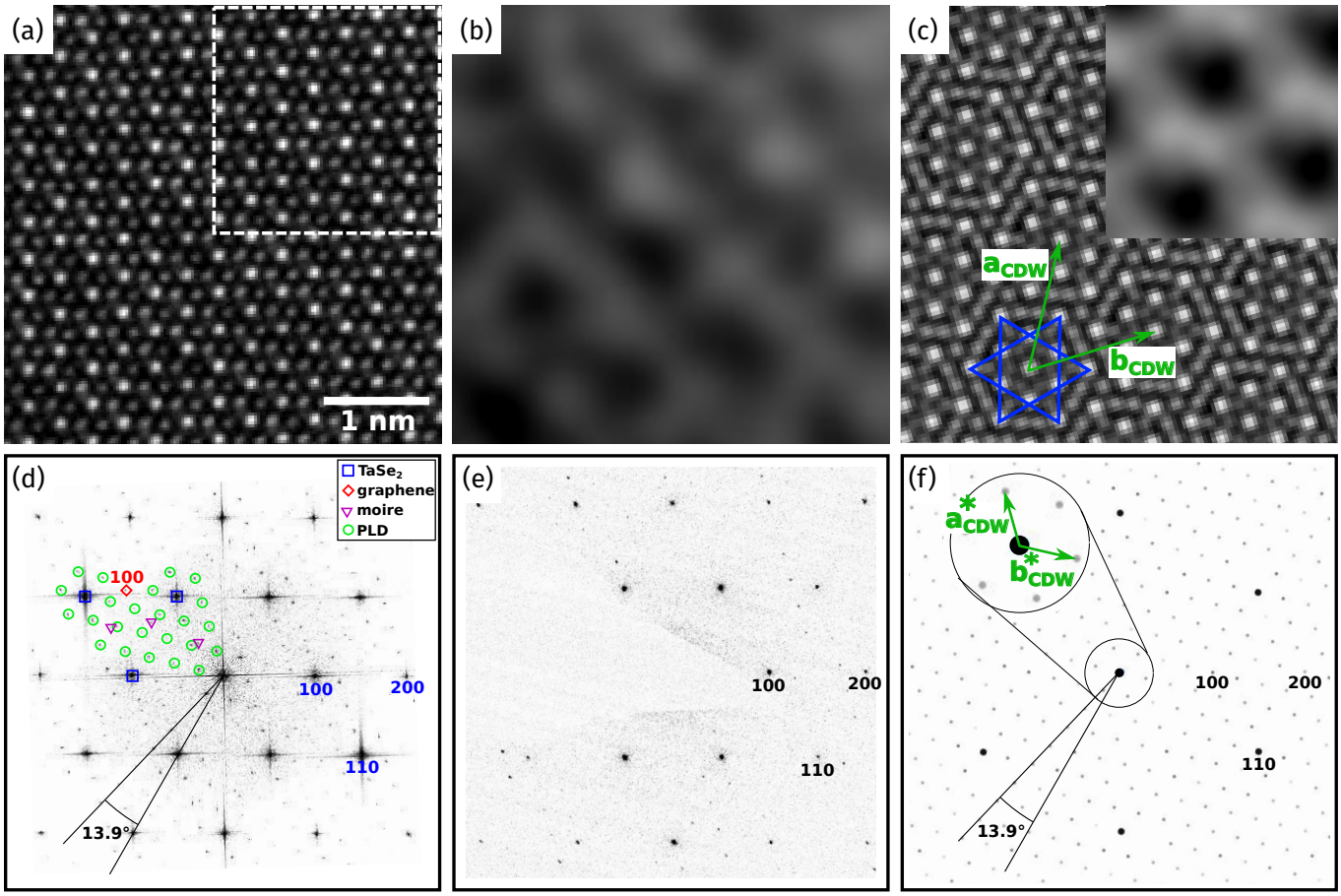

FIG. 3. (a) Experimental AC-HRTEM image of the 1T-$TaSe_2$ - graphene heterostructure at 80 kV. Ta atoms show a higher contrast than Se atoms. In the upper right corner the graphene lattice is filtered out, which does not show a difference to the unfiltered image. (b) To visualize the contrast variation due to the CCDW/PLD, a Gaussian blur is applied on the image reducing only high-frequency information. (c) Simulated AC-HRTEM image of the CCDW/PLD in a single 1T-$TaSe_2$ layer. The star-of-David is marked in blue and the superstructure lattice vectors $\mathbf{a_{CDW}}$ and $\mathbf{b_{CDW}}$ in green. In the inset the Gaussian blur is applied to the image and reveals quantitatively the same contrast variation as found in the experimental image (b). The Fourier transformation (d) of the experimental AC-HRTEM image (a) shows satellite spots (green) as well as 1T-$TaSe_2$ reflections (blue), graphene reflections (red) and reflections of the Moiré-pattern between graphene and 1T-$TaSe_2$ (pink). The satellite spots are rotated about 13.9° against the 100 1T-$TaSe_2$ reflections, identifying the structure as commensurate. In the SAED pattern of the 1T-$TaSe_2$ monolayer on graphene (e), satellite spots of the CCDW/PLD are visible. (f) Simulated kinematic electron diffraction pattern of the CCDW/PLD in single 1T-$TaSe_2$ layer. It shows satellite spots as well as the rotation angle for the commensurate superstructure. In the enlarged area reciprocal lattice vectors of the superstructure $\mathbf{a^*_{CDW}}$ and $\mathbf{b^*_{CDW}}$ are shown.

has already been transferred (see Figure 2 (d)). The Au sputtered grids show better heat conductivity during cooling experiments, but they have the disadvantage of a very low contrast for monolayers in the optical microscope. A 1T-$TaSe_2$ / graphene heterostructure was prepared to reduce electron beam-induced damages of the 1T-$TaSe_2$ layer[27–29] during the HRTEM investigations. Furthermore, graphene acts as a support material for the few micrometer wide monolayers.

The experimental HRTEM image of the 1T-$TaSe_2$/graphene heterostructure is presented in Figure 3 (a). Due to the low contrast of graphene, the contrast is dominated by the 1T-$TaSe_2$ structure. We chose Scherzer defocus imaging conditions and Ta (180.95 u) atoms have a higher contrast than Se (78.96 u) atoms due to their higher atomic mass. In the upper right corner of Figure 3 (a) the graphene lattice is filtered out. This filtered inset does not show a visible difference to the unfiltered rest of Figure 3 (a). A contrast variation in the HRTEM image due to the CCDW/PLD can be revealed by reducing high frequency information of the lattice in the image. This is realized by a convolution with a Gaussian function with an appropriate radius of decay (Gaussian high-low pass filter function of Digital Micrograph[34]). The filtered image reveals a pronounced contrast variation (see Figure 3 (b)). To show that this contrast variation originates from the commensurate $\sqrt{13}$-superstructure, a HRTEM image with the

DFT-relaxed superstructure of the 1T-$TaSe_2$ monolayer is simulated (see Figure 3 (c)). The simulated HRTEM image shows a pronounced star-of-David-like superstructure. One example of a star-of-David is marked in blue, as well as the superstructure lattice vectors $\mathbf{a_{CDW}}$ and $\mathbf{b_{CDW}}$ in green. The experimental HRTEM image (Figure 3 (a)) shows a less distinctive contrast modulation of the Ta and Se atoms in comparison to the simulated superstructure image (Figure 3 (c)). In the upper right corner of Figure 3 (c) a Gaussian blur is applied on this part of the simulated image. The images with Gaussian blur have quantitatively the same contrast modulation (Figure 3 (b) and (c)) which indicates once again that the experimentally found superstructure is the expected $\sqrt{13}$-superstructure. To validate the superstructure, we analyzed it in the reciprocal space. The Fourier transformed pattern of the HRTEM image is depicted in Figure 3 (d), which reveals the main 1T-$TaSe_2$ reflections, marked in blue, satellite spots due to the $\sqrt{13}$-superstructure, marked in green and graphene reflections, marked in red. Reflections originating from a convolution between the graphene and the 1T-$TaSe_2$ structure are marked in pink. As can be seen, the satellite spots are rotated about 13.9° against the 100 reflection, which proves that the superstructure is commensurate with the underlying lattice. Furthermore a selected area electron diffraction (SAED) pattern originating from a larger sample area shows the main reflections of the 1T-structure and satellite spots of the $\sqrt{13}$-superstructure (see Figure 3 (e)). Reflections of the graphene lattice are not visible as they have a much smaller intensity than the 1T-$TaSe_2$ reflections. For the sake of completeness a simulated kinematic electron diffraction pattern is shown in Figure 3 (f), showing the reflections of the 1T-$TaSe_2$ structure and satellite spots due to the $\sqrt{13}$-superstructure. In the enlarged area the reciprocal lattice vectors of the superstructure $\mathbf{a^*_{CDW}}$ and $\mathbf{b^*_{CDW}}$ are shown which have the length of $|\mathbf{a^*_{CDW}}| = |\mathbf{b^*_{CDW}}| = 1/(\sqrt{13}\, a_0)$. The angle between the satellite spots and the main 100 reflections is 13.9°. The positions of the 1T-$TaSe_2$ reflections and satellite spots in the experimental Fourier transformation and the SAED pattern are the same as in the simulated diffraction pattern. This all identifies the superstructure in the single-layer 1T-$TaSe_2$ sample as the expected $\sqrt{13}$-superstructure however the experimental HRTEM image shows a less pronounced star-of-David-like contrast modulation. This structure is formed at about room temperature which confirms the assumed temperature behavior from bulk crystals down to monolayers.[23]

The stability of the CCDW/PLD in a single-layer of 1T-$TaSe_2$ is predicted by density functional theory (DFT) relaxations which shows the same superstructure for a single-layer 1T-$TaSe_2$ as known for bulk 1T-$TaSe_2$. To see whether the graphene substrate has an influence on the 1T-$TaSe_2$ layer, we performed calculations of the CCDW/PLD phase on graphene, as described in detail below. In the alignment of Fermi levels of the systems, the graphene substrate will donate electrons to the 1T-$TaSe_2$ sheet, as shown in Figure 4 (a), but this does not result in any noticeable alterations of the CCDW/PLD structure. Although charge transfer between the 1T-$TaSe_2$ and the graphene layer does not completely destabilize the CCDW/PLD phase, it might affect its formation energy. To investigate this, we carried out a series of calculations with account for doping of the CCDW/PLD and the undistorted phase with a series of different fractional electron charges, computing the CCDW/PLD formation energy per formula unit as $E_f = E(\text{Pristine}) - \frac{E(\text{CCDW/PLD})}{13}$, thus defined as the positive energy gained by the structure upon distortion. The results, for a range of large, but possibly realizable surface electron charges is shown in Figure 4 (b). The CCDW/PLD is further stabilized by electron doping (increasing formation energy), whereas hole doping tends to decrease the formation energy, although -at realistic doping concentrations- not enough to stabilize the undistorted phase. The sudden downturn of the formation energy curve in Figure 4 (b) around 7.5 x 10^{13} electrons/cm^2 results from the complete filling of one additional, isolated empty band in the CCDW/PLD structure.

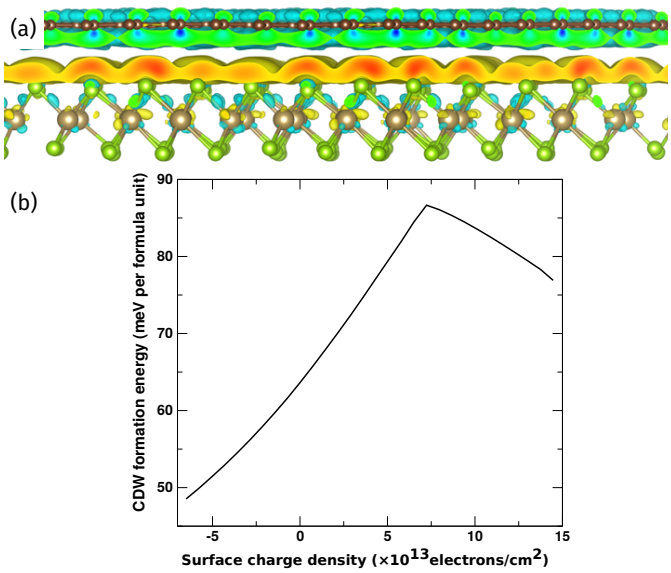

FIG. 4. (a) Illustration of the charge transfer from graphene to 1T-$TaSe_2$. Green/blue areas illustrate electron depletion and red/yellow areas electron accumulation, as compared to isolated layers. (b) Formation energy of the CCDW/PL as function of the surface charge density, in electrons per cm^2.

To sum up, we have unambiguously proven that the CCDW/PLD is stable in a monolayer of 1T-$TaSe_2$ at room temperature. We have shown that the expected commensurate $\sqrt{13}$-superstructure has been formed as we investigated not just the monolayer of 1T-$TaSe_2$ but the heterostructure consisting of two monolayers (1T-$TaSe_2$ and graphene). We conclude that the underlying graphene has no influence on the commensurate $\sqrt{13}$

PLD in a monolayer of 1T-$TaSe_2$.

See supplementary material for experimental details.

The authors acknowledge financial support by the German research foundation (DFG) and the Ministry of Science, Research and the Arts (MWK) of Baden-Württemberg in the frame of the "SALVE" (Sub Angstrom Low-Voltage Electron microscopy) project and project KR 4866, as well as by the EU in the frame of the Graphene Flagship. A. V. K. also thanks the Akademy of Finland for the support under Project No. 286279. We acknowledge CSC Finland and PRACE (HLRS, Stuttgart, Germany) for generous grants of CPU time.

[1] K. S. Novoselov, Z. Jiang, Y. Zhang, S. Morozov, H. L. Stormer, U. Zeitler, J. Maan, G. Boebinger, P. Kim, and A. K. Geim, Science **315**, 1379 (2007).
[2] B. Keimer, S. A. Kivelson, M. R. Norman, S. Uchida, and J. Zaanen, Nature **518**, 179 (2015).
[3] J.-F. Ge, Z.-L. Liu, C. Liu, C.-L. Gao, D. Qian, Q.-K. Xue, Y. Liu, and J.-F. Jia, Nature materials **14**, 285 (2015).
[4] J. A. Wilson, F. J. Di Salvo, and S. Mahajan, Advances in Physics **24**, 117 (1975).
[5] K. Rossnagel, Journal of physics. Condensed matter : an Institute of Physics journal **23**, 213001 (2011).
[6] T. Uchihashi, Superconductor Science and Technology **30**, 013002 (2016).
[7] R. E. Peierls, *Quantum theory of solids*, 23 (Oxford University Press, 1955).
[8] A. Overhauser, Advances in Physics **27**, 343 (1978).
[9] J. Freidel, *Electron-phonon interactions and phase transitions*, edited by T. Riste, Vol. 29 (Springer Science & Business Media, 1977).
[10] M. Chhowalla, H. S. Shin, G. Eda, L.-J. Li, K. P. Loh, and H. Zhang, Nature chemistry **5**, 263 (2013).
[11] J. A. Wilson and A. D. Yoffe, Advances in Physics **18**, 193 (1969), http://dx.doi.org/10.1080/00018736900101307.
[12] K. S. Novoselov, A. K. Geim, S. V. Morozov, D. Jiang, Y. Zhang, S. V. Dubonos, I. V. Grigorieva, and A. Firsov, Science **306**, 666 (2004).
[13] K. Novoselov, D. Jiang, F. Schedin, T. Booth, V. Khotkevich, S. Morozov, and A. Geim, Proceedings of the National Academy of Sciences of the United States of America **102**, 10451 (2005).
[14] G.-H. Lee, Y.-J. Yu, X. Cui, N. Petrone, C.-H. Lee, M. S. Choi, D.-Y. Lee, C. Lee, W. J. Yoo, K. Watanabe, *et al.*, ACS nano **7**, 7931 (2013).
[15] Q. H. Wang, K. Kalantar-Zadeh, A. Kis, J. N. Coleman, and M. S. Strano, Nature nanotechnology **7**, 699 (2012).
[16] D. Jariwala, V. K. Sangwan, L. J. Lauhon, T. J. Marks, and M. C. Hersam, ACS nano **8**, 1102 (2014).
[17] D. Sakabe, Z. Liu, K. Suenaga, K. Nakatsugawa, and S. Tanda, npj Quantum Materials **2**, 22 (2017).
[18] X. Xi, L. Zhao, Z. Wang, H. Berger, L. Forró, J. Shan, and K. F. Mak, Nature nanotechnology **10**, 765 (2015).
[19] M. Bovet, D. Popović, F. Clerc, C. Koitzsch, U. Probst, E. Bucher, H. Berger, D. Naumović, and P. Aebi, Physical Review B **69**, 125117 (2004).
[20] J.-A. Yan, M. A. D. Cruz, B. Cook, and K. Varga, Scientific reports **5**, 16646 (2015).
[21] M.-T. Suzuki and H. Harima, Journal of Magnetism and Magnetic Materials **272**, E653 (2004).
[22] P. Darancet, A. J. Millis, and C. A. Marianetti, Physical Review B **90**, 045134 (2014).
[23] R. Samnakay, D. Wickramaratne, T. R. Pope, R. K. Lake, T. T. Salguero, and A. A. Balandin, Nano letters **15**, 2965 (2015).
[24] M. Mirjalili and J. Vahdati-Khaki, Journal of Physics and Chemistry of Solids **69**, 2116 (2008).
[25] H.-P. Komsa, J. Kotakoski, S. Kurasch, O. Lehtinen, U. Kaiser, and A. V. Krasheninnikov, Physical review letters **109**, 035503 (2012).
[26] R. Egerton, P. Li, and M. Malac, Micron **35**, 399 (2004).
[27] T. Lehnert, O. Lehtinen, G. Algara-Siller, and U. Kaiser, Applied Physics Letters **110**, 033106 (2017).
[28] G. Algara-Siller, S. Kurasch, M. Sedighi, O. Lehtinen, and U. Kaiser, Applied Physics Letters **103**, 203107 (2013).
[29] R. Zan, Q. M. Ramasse, R. Jalil, T. Georgiou, U. Bangert, and K. S. Novoselov, ACS nano **7**, 10167 (2013).
[30] A. A. Balandin, S. Ghosh, W. Bao, I. Calizo, D. Teweldebrhan, F. Miao, and C. N. Lau, Nano letters **8**, 902 (2008).
[31] P. Börner, U. Kaiser, and O. Lehtinen, Physical Review B **93**, 134104 (2016).
[32] M. M. Benameur, B. Radisavljevic, J. S. Heron, S. Sahoo, H. Berger, and A. Kis, Nanotechnology **22**, 125706 (2011).
[33] P. Blake, E. W. Hill, A. H. C. Neto, K. S. Novoselov, D. Jiang, R. Yang, T. J. Booth, and A. K. Geim, Applied Physics Letters **91**, 063124 (2007).
[34] *Gatan Inc.'s Digital Micrograph*.